# N00014-19-1-2213

# Nanoparticle-based Optical Components and Coatings (NOCC)

## Final Research Performance Progress Report

29 April 2024

**Submitted to:**

Dr. Antti Makinen
NAVAL MATERIALS & MANUFACTURING DIV
875 N. Randolph Street
Arlington VA 22203-1995
email: antti.j.makinen.civ@navy.mil

**Submitted by:**

**The Charles Stark Draper Laboratory, Inc.**
CAGE Code: 51993
DUNS Number: 06-658-7478

**Technical Point of Contact**
David J. Carter, Ph.D.
Phone: (617) 258-2079
email: davidc@draper.com

**Contractual Point of Contact**
Mr. John Hammett
Phone: (617) 258-4146
email: jhammett@draper.com

## Major Goals

This goal of this program is to explore fabricating optical components and coatings using substrate-bound formations (crystals) of DNA-nanoparticle (DNA-NP) superlattices (Figure 1). While the fundamental science of making these complex assemblies in solution was well-understood at the beginning of this effort, the optical properties of the structures, and their relation to assembly conditions, was largely unknown.

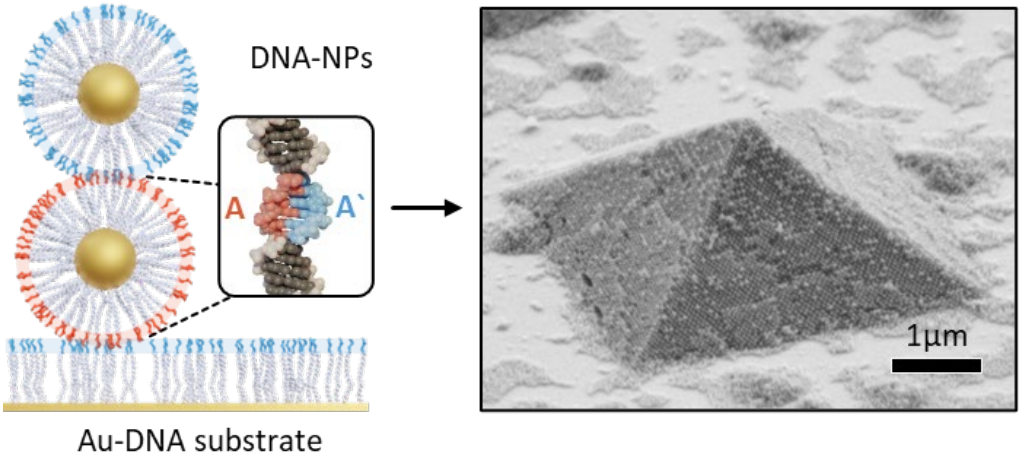


Figure 1: Left: DNA can be used to assemble nanoparticles into crystals with defined habits and crystal orientations through the DNA interaction. Right: SEM image of micron-scale BCC crystal with <100> orientation on a substrate..

This work leveraged our previous results in growing truncated Wolff polyhedra (Winterbottom structures) on substrates to use their facets as mirrors, which could be used to route optical signals from in-plane to out-of-plane and vice-versa to enable interchip optical communication in optical multichip modules (Figure 2).

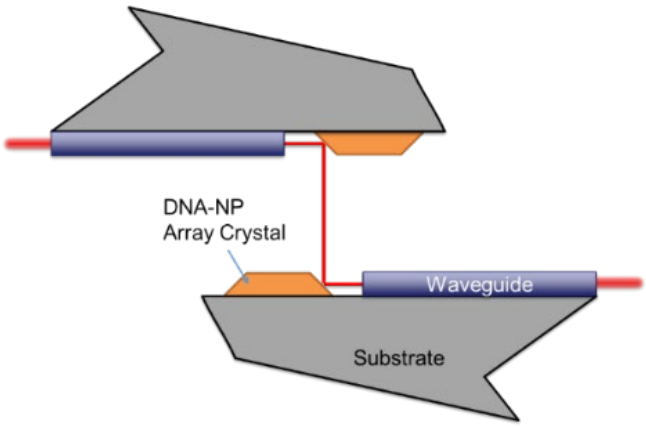


Figure 2: Schematic of proposed demonstration of interlevel optical signal steering using assembled DNA-NP array mirrors.

We have optimized conditions to controllably grow these structures on surfaces and characterized their optical properties. We have investigated the physics of crystal assembly on the surface to understand the impact of patterning of the substrate to develop techniques to grow crystals of a pre-determined size, shape, orientation, and placement. With this knowledge, we have designed a process and developed designs for chips with optical waveguides with mirrors grown at their end facets. Future work could fabricate these devices to demonstrate coupling of light on and off the chip.

Our longer-term goal will be to use self-assembly to control the optical index as a function of position (height above the substrate and laterally) so we could, for example, create index matching structures to minimize reflections, or multilayer mirrors over large non-flat areas.

## Accomplishments Under Goals

This program has consisted of three main sequential efforts: (1) optical measurements on single crystal facets and demonstrating their use as optical mirrors to direct light into an optical fiber, (2) studying growth conditions to reliably grow single crystals to a defined size, shape, and orientation on a precise predefined location on the substrate, and (3) developing a microfabrication process and designs to build waveguides with integrated self-assembled crystals to demonstrate off-chip optical coupling.

### Optical Measurements on Single Crystals:

We present data that includes specularity and side-facet-angle measurements on retroreflection from crystals, a demonstration of coupling light from a microscope through the crystal facet mirror to an optical fiber, and measurements of reflectivity both with and without coatings on the crystals.

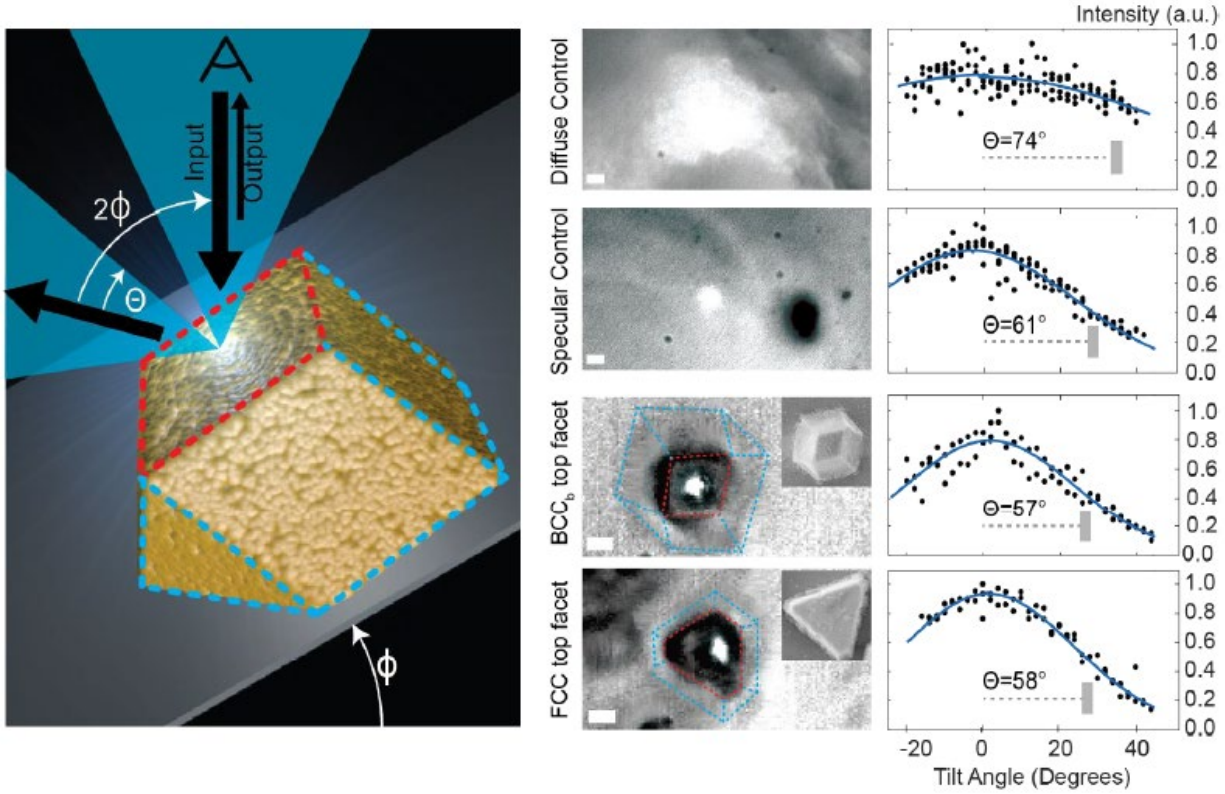


Figure 3: Retroreflection measurements of Winterbottom crystallite top facets. The scheme (left) demonstrates how the retroreflection setup as a function of substrate tilt is used to measure beam divergence. Optical images during measurement (middle) illustrate the incident spot size focusing onto the top facet (outlined in red) of the crystallite structure (outlined in blue), with SEM insets included for clarity. The retroreflection intensity profile (right) demonstrates that BCC and FCC structures retain specular retroreflection profiles, quantified by the divergence angle matching the Si wafer specular control, indicating high-quality mirror surfaces. For clarity, Θ/2 is visualized (grey bar). Scale bars are 2μm, with SEM inset scale matched to optical image scale.

Due to the small (~4 μm) facet size of the crystals, converging light from a microscope must be used to make reflection measurements. A Nikon Ti2 Dual-Deck microscope was used to characterize scattering from crystal faces and compare their specularity to silicon mirrors and diffuse (paper) controls. Retroreflection measurements across a range of incident angles were conducted using a 450 nm wavelength laser and a eucentric stage. The specularity of the surface was assessed by measuring the change between the divergence of the incident beam and the outgoing beam divergence. If the two beam divergences are approximately equal, the surface is qualitatively specular, while if the outgoing beam divergence is significantly larger, the surface is diffuse. The beam divergence from the silicon control was measured to be 61° degrees, approximately matching the expected value of 64° from our 0.9NA microscope setup. In contrast, the diffuse paper control had a beam divergence of 74°. The reflections from FCC and BCC crystal facets were measured to be 58° and 57°, respectively, equivalent to the silicon specular control (see Figure 3).

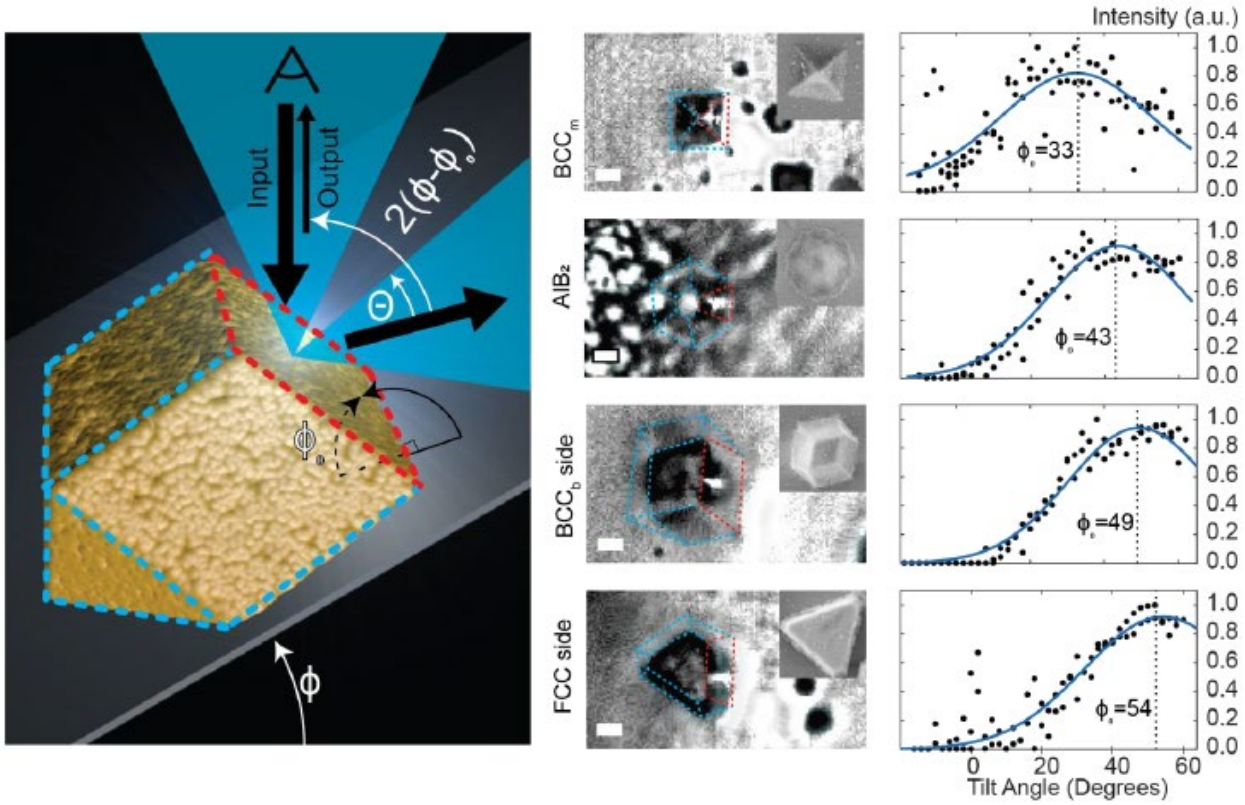


Figure 4: Retroreflection measurements of Winterbottom crystallite side facets on BCCm, BCCb, FCC, and AlB2 structures. The scheme (left) demonstrates how the retroreflection setup as a function of substrate tilt is used to measure beam divergence. Optical images during measurement (middle) illustrate the incident spot size focusing onto the side facet (outlined in red) of the crystallite structure (outlined in blue), with SEM insets included for clarity. The retroreflection intensity profile (right) demonstrates that the side facets retain specular profiles, and that the offset due to facet tilt matches the trends of facet angle predicted from the Winterbottom construction. Scale bars are 2μm, with SEM inset scale matched to optical image scale.

Additionally, facet angles of different crystal structures can be discerned with retroreflection from the side facets of these crystals. As shown in Figure 4, the facet angles from a BCC[100]

AlB2, BCC[110], and FCC were measured to be 33°, 44°, 49°, and 54°. These values match the trend of expected values from the predicted crystal facets (45°,54°,60° and 71°), although all are smaller than anticipated. This discrepancy can be attributed to secondary reflections into and scattering from the substrate that would skew the measured value towards the substrate normal.

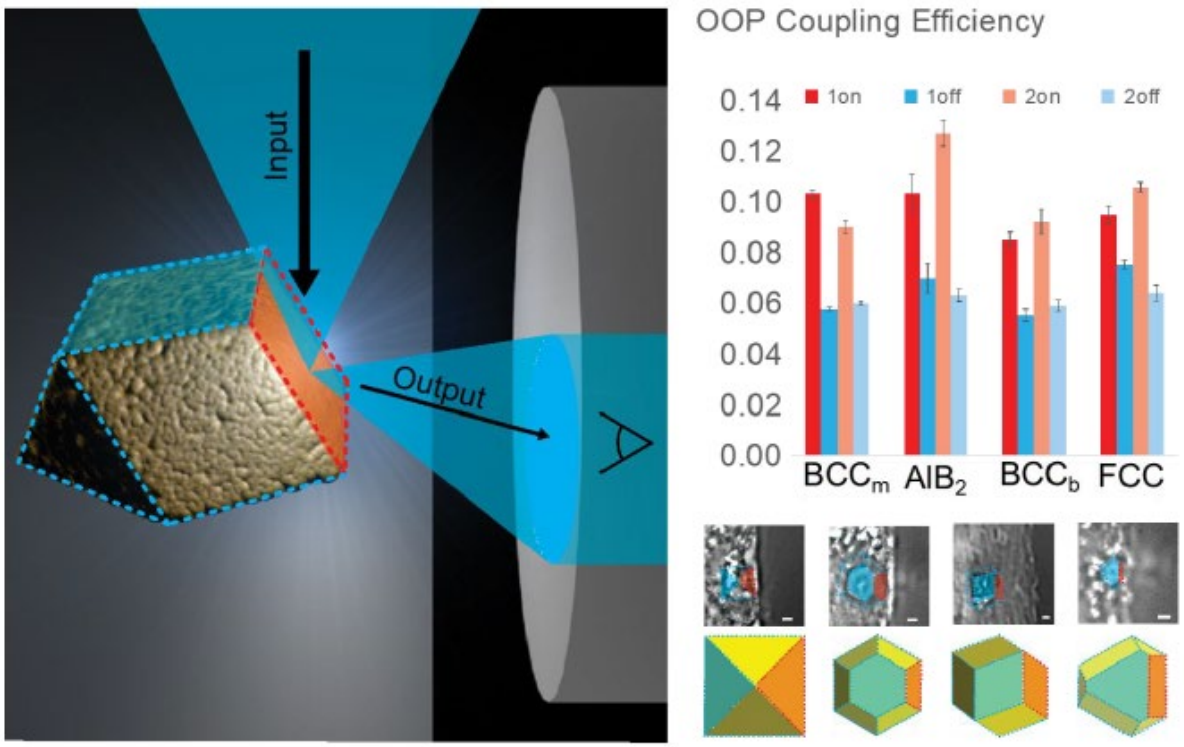


Figure 5: Out-of-plane coupling efficiency measurement for BCCm, BCCb, FCC, and AlB2 structures. Scheme (left) demonstrates how out-of-plane measurements were taken using an optical fiber probe. The out of plane coupling efficiency was measured for two crystals (right bottom) for both on-target setups (red facets, bars) and compared against measurements aimed off-target (blue facets, bars), corresponding to non-specular scattering of the laser off the surface. The difference between on-target and off-target measurements is attributed to specular facet reflections.

To demonstrate that crystals can act as micromirrors, direct measurement of out-of-plane coupling of light into an optical fiber was performed. In order to find the optimal placement of the optical fiber, align it with the crystal, and prevent interference, the substrate had to be removed to within a few micrometers of the crystal. A combination of polishing and focused-ion-beam (FIB) was used to remove the substrate in the vicinity of a crystal of interest. Optical power was observed to reflect into the fiber when the objective was aimed at the appropriate crystal facet, confirming that the crystals are capable of acting as micromirrors. Off-target facets were found to have significantly lower reflection into the fiber, as shown in Figure 5.

Coupling efficiencies were low in the aforementioned measurements; this is unsurprising given that the nanoparticles are gold which has strong absorption at the wavelength of interrogating light (450 nm), preventing most of the light from reflecting into the optical fiber. To increase the reflectivity at this wavelength, the crystals were coated with 100 nm of Ag using atomic layer

deposition. Measurements repeated after this coating show a very high coupling efficiency, reaching 85% for the BCC[110] crystal type (see Figure 6).

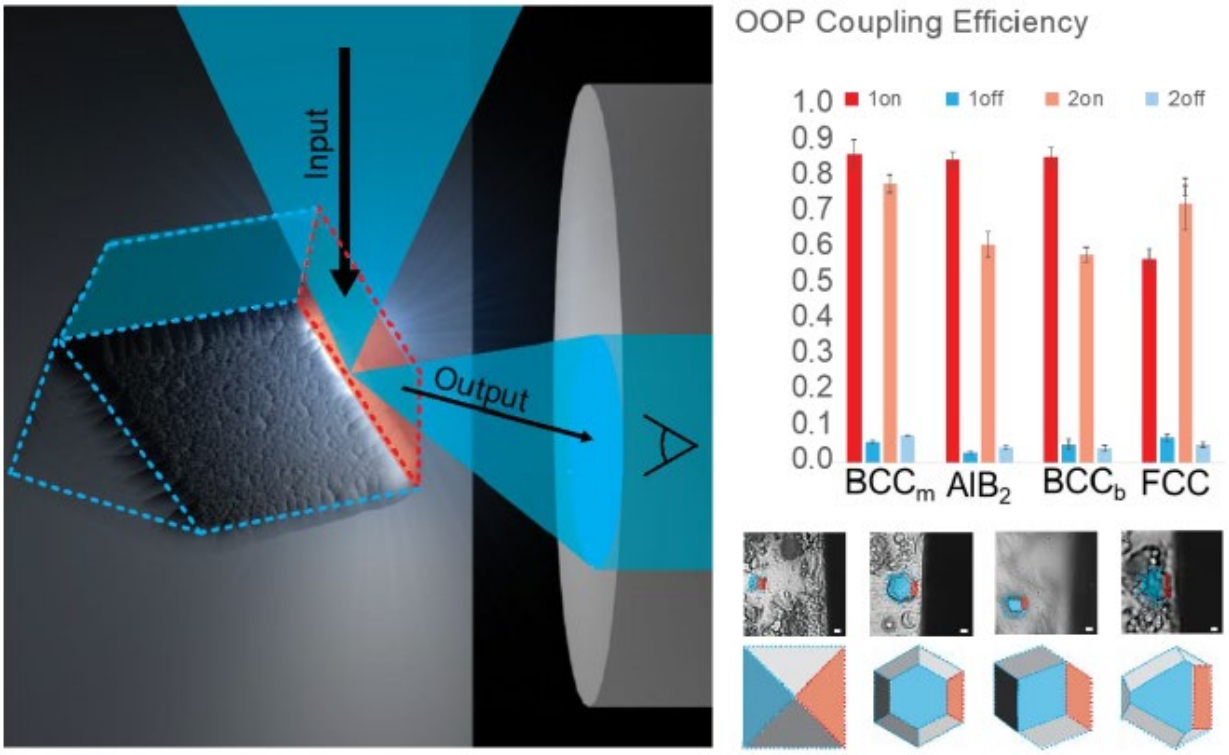


Figure 6: Out-of-plane coupling efficiency measurement for BCCm, BCCb, FCC, and AlB2 structures after reflective coating. Scheme (left) demonstrates how out-of-plane measurements were taken using an optical fiber probe. The out of plane coupling efficiency was measured for two crystals (right bottom) for both on-target setups (red facets, bars) and compared against measurements aimed off-target (blue facets, bars), corresponding to non-specular scattering of the laser off the surface. The difference between on-target and off-target measurements is attributed to specular facet reflections. OOP coupling increases significantly after Ag deposition, attributed to increased reflectivity while retaining the desired tilted-mirror geometry.

**Growth of Crystals with Predefined Position, Size, and Orientation:**

Once the ability to use crystals as micromirrors was confirmed, we studied the growth of crystals on patterned substrates with the goal of growing crystals with precise placement and orientation to enable their use in optical devices. The structure/shape of the crystals in this study was predefined by the DNA choice to be BCC oriented in the [100] plane, creating pyramid structures.

The DNA used to build the crystals is bound to the gold nanoparticles and the gold-coated substrate through a thiol group (gold-thiol bond). To grow crystals in certain locations, the DNA anchors must only attach in certain regions; this requires either isolated gold patches or for the gold to be covered. For all work described here, silicon substrates were coated in gold (ebeam evaporation, 2 nm Cr adhesion layer, 8 nm gold), then coated with a 1µm thick photoresist

(AZ3312 positive resist). The resist was removed in patterned regions to expose the gold substrate at the bottom of photoresist wells, as shown in Figure 7.

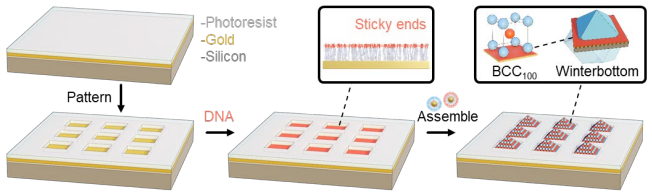


Figure 7: Approach to use photoresist-patterned substrates to grow self-assembled Winterbottom crystals in defined locations on the substrate.

Initially, issues with nonspecific adsorption of DNA-NPs to the photoresist masked crystal growth behavior in the wells. The use of surfactants, in particular 0.34 mM SDS (sodium dodecyl sulfate) sufficiently blocked DNA-NP adsorption to the photoresist, allowing growth to commence in the wells.

Patterns were designed to explore the effect of size and density of the wells on crystal growth. Using standard deposition conditions (20nM NP concentration, 1.5M NaCl in PBS, slow cooling from 65°C to 25°C at 0.1°C/min), the size and density of the wells was varied to determine how they affect crystal nucleation. As shown in Figure 8A and C, increasing well size from 1.5 µm to 6 µm at 12 µm pitch increases the frequency of crystals nucleating in the wells. At the smallest size, only 20% of the wells nucleated crystals, while at the largest size, multiple nucleation events resulted in polycrystalline structures. The optimum well size for generating single crystals at 12 µm pitch was 4 µm.

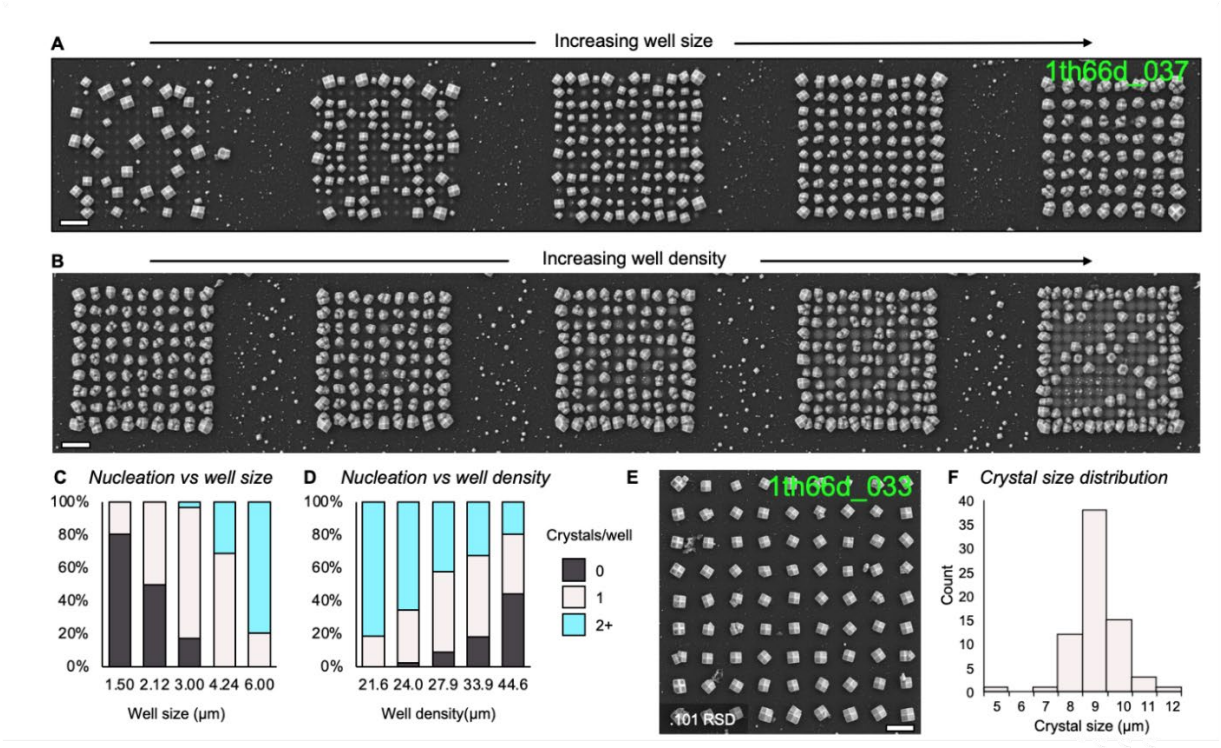


Figure 8 – A, C) Increasing well size increases nucleation events, maximizing single crystal formation at a well size of approximately 4 µm. B, D) Increasing well density decreases nucleation events as wells compete with each other for DNA-NP supply. E, F) Using appropriately sized and spaced arrays allows for monodisperse single crystal formation. Scale bars are 20 µm.

Because DNA-NPs migrate on the surface to the wells for crystal growth, nearby wells compete for resources. Patterns with the same size wells at increasing well density showed decreasing nucleation events and uneven crystal size (crystals on the outside of the pattern were larger than on the central wells) as well density increased (Figure 8 B and D). This suggests there is a minimum distance required between wells to ensure that they are independent of each other. Crystals grown in wells at sufficiently large spacings (~30 µm for 6 µm wells) have a monodisperse, well defined size (Figure 8 E and F).

Altering the size of the crystals can be done by altering growth conditions; size can be doubled (from 6 µm to 12 µm face width) by halving the cooling rate, however further research needs to be done on the silica embedding process of crystals of this size. With larger crystals it became apparent that the current embedding process only penetrates a few micrometers into the crystal, creating a shell structure that collapses upon drying. Additionally, the growth of larger crystals increases the required spacing between wells to eliminate competition and requires re-optimization of pattern spacing.

To orient crystals, several pattern choices were explored. It was hypothesized that square wells would cause crystal orientation to the walls of the well, and 'feeder' lines could help funnel particles towards growth nodes. A particularly promising pattern was one that had a series of crosshatches, where growth would occur at nodes and be oriented by the feeder lines. Figure 9 shows measurements of orientation with no patterning (A), in square wells (B, D), and on crosshatches (C, E), demonstrating that crosshatches have a preferred orientation to the crystals.

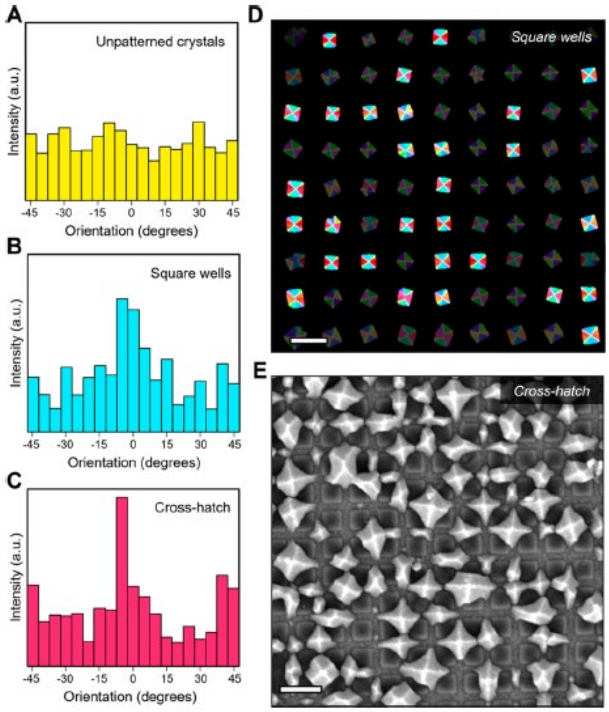


Figure 9: Orientation control by patterning. Unpatterned crystals (A) show unform distribution of angle. Square wells (B, D) show preference towards 0 degree and 45-degree orientation. Cross-hatch patterns (C, E) show more uniform 0-degree orientation. Scale bars are 20 µm.

**Fabrication Process and Design of Structure for Off-chip Optical Coupling Demonstration:**

With the ability to position and orient crystals, we turned to developing a waveguide/crystal co-fabrication process to enable a demonstration of coupling light into on-chip waveguides using self-assembled mirrors. We leveraged Draper silicon nitride ($SiN_x$)waveguide designs.

We first explored the possibility of coupling light from a $SiN_x$ waveguide directly onto a mirror. As shown in Figure 10, with typical minimum dimensions of ~0.3 µm, the expansion angle of the expanding mode calculated using Gaussian beam expansion is too large to hit the mirror.

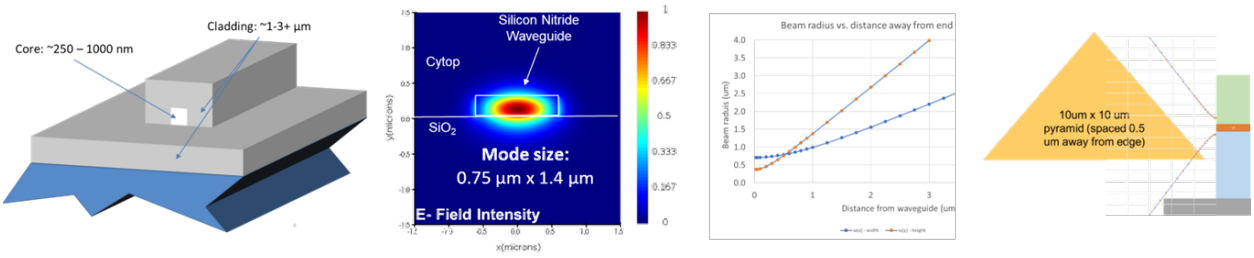


Figure 10 – Left: typical $SiN_x$ waveguide dimensions and simulated mode size in a 0.3 µm x 1.2 µm waveguide. Right: calculated mode expansion overlaid which schematic of mirror in front of waveguide showing that the numerical aperture of the expanding mode is so large that the majority of the light will miss the mirror.

This is a similar problem to what is encountered when trying to couple light from an optical fiber into an on-chip waveguide. A common solution for that is to use edge couplers that consist of a larger high-index material (commonly photopatternable SU-8 epoxy) on top of the edge of the waveguide. The mode then expands from the nitride into the SU-8 and has a lower expansion angle. This approach should be applicable to our mirrors, as shown in Figure 11.

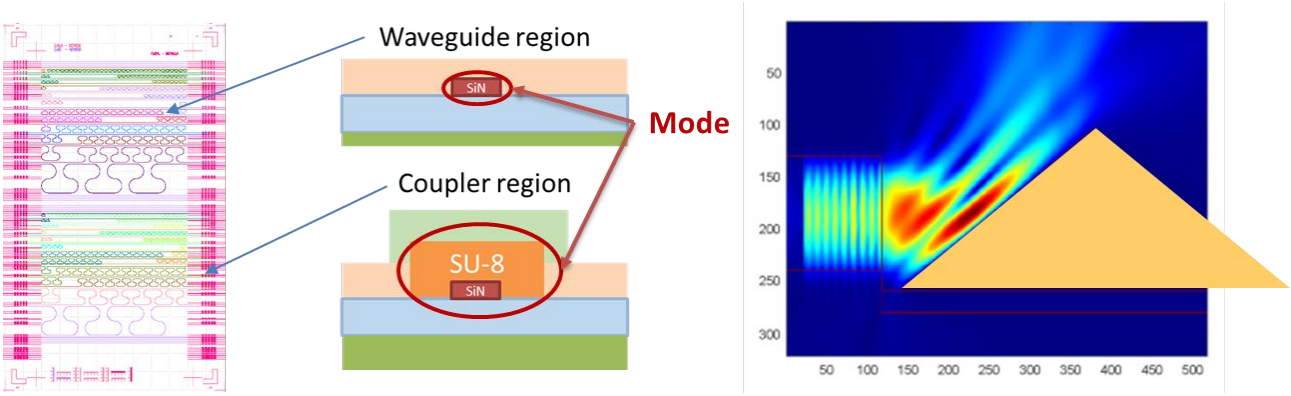


Figure 11 – Left: Layout of $SiN_x$ waveguide structures with optical couples (pink) at edges of chip. Center: comparison of mode sizes in the waveguide and coupler. Right: Finite-difference time-domain simulation of light expanding from an SU_8 coupler onto mirror showing the majority of the light hits the mirror.

We have designed a microfabrication process to co-fabricate waveguides with couplers and self-assembled mirrors. Figure 12 illustrates a simplified side view of the process. Figure 12A shows the base substrate of silicon with an oxide later. The oxide layer is patterned as shown in figure 12B, then an additional oxide is deposited to create a step in the oxide as shown in figure 12C. In figure 12D, gold is patterned onto the lower step of the oxide using a liftoff process. Figure 12E shows the patterning of the SU-8 waveguide structure up to the edge of the oxide step. Figure 12F shows a patterned fluoropolymer coating (CYTOP) that is used for mechanical protection of the waveguide and to improve optical performance.

The waveguide structure is now complete; subsequent steps prepare the pattern for self-assembly of the mirror. Figure 12G shows patterned photoresist with an opening to the gold for crystal growth. Figure 12H shows the crystal grown in the well along with gold deposited on the photoresist. Figure 12I shows the final structure after the photoresist is removed along with the gold that was on top of it.

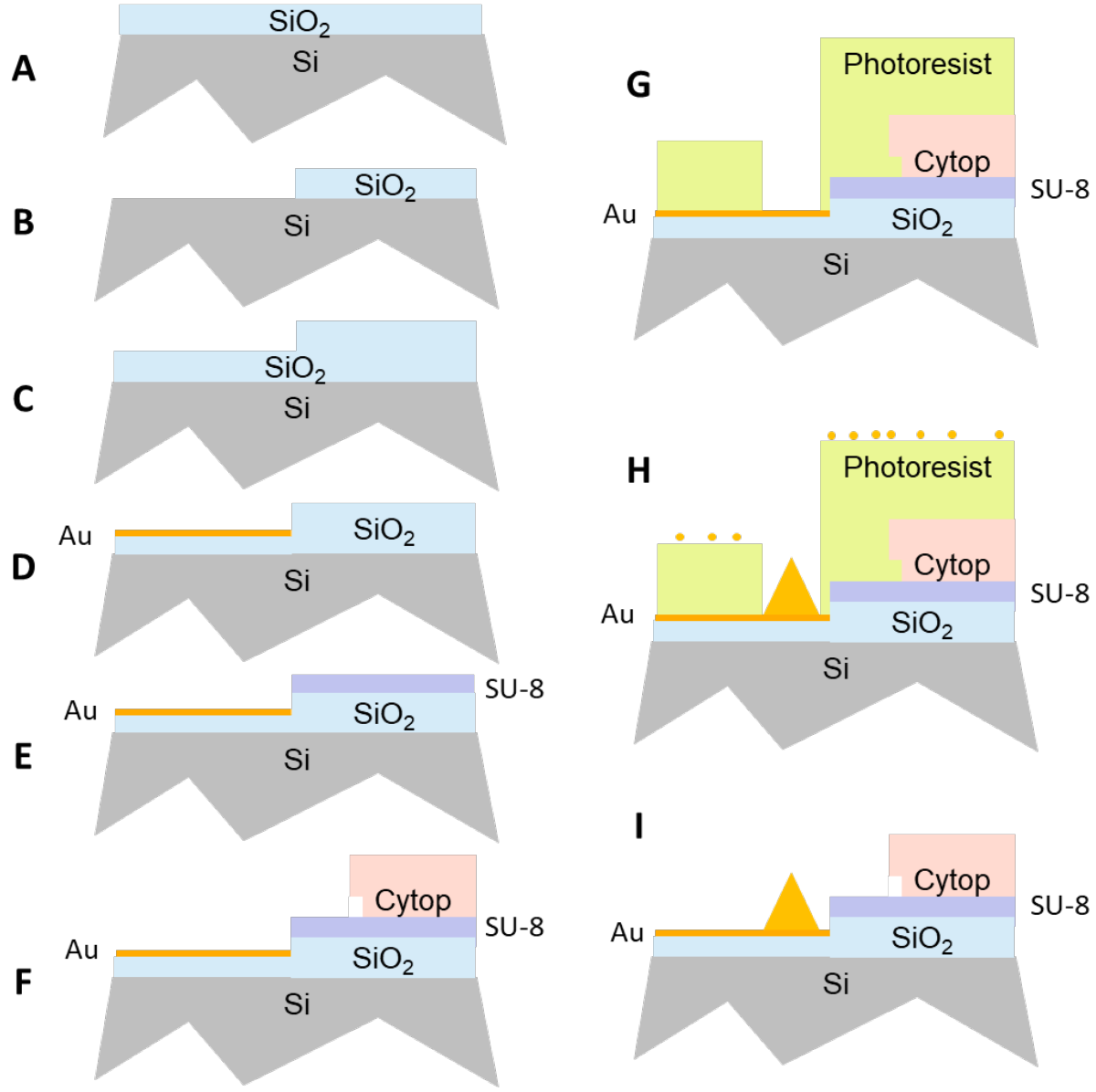


Figure 12 – Process flow for co-fabrication of waveguides and self-assembled mirrors. Detailed descriptions of individual steps are in the text.

We have designed photomasks for this process flow and have done preliminary experiments to optimize individual process steps. This has essentially cleared the ground for completing a demonstration device.

## Future Plans

An obvious next step in this work would be to complete the demonstration of self-assembled coupling mirrors for off-chip optical coupling.

Beyond that, extension of self-assembly of metallic nanoparticles to dielectrics and other materials opens up the possibility of making larger constructs such as conformal coatings that would permit optical lensing, waveguiding, or more sophisticated optical behaviors such as perfect retroreflection or even optical cloaking.

A next step would be to establish the basic design principles and synthesis methods needed to achieve these more complex optical materials by developing experiments to understand the basic physics of conformal film formation and extending our metallic nanoparticle/gold substrate assembly process to a wider variety of nanoparticles and substrate materials (in particular dielectric NPs).

## Results Dissemination

Lewis, D. J., Zornberg, L. Z., Carter, D. J. D., & Macfarlane, R. J. "Single Crystal Winterbottom Constructions of Nanoparticle Superlattices," *Nature Materials.* **19***,* 719–724 (2020)

Lewis, D. J., Carter, D. J. D., & Macfarlane, R. J. "Using DNA to Control the Mechanical Response of Nanoparticle Superlattices," *JACS.* **142, 45**, 19181–19188 (2020)

Pashuck, E.T., Seeman, N. & Macfarlane, R. Self-assembly of bioinspired and biologically functional materials. *MRS Bulletin* **45,** 832–840 (2020)

Leonardo Z. Zornberg, Diana J. Lewis, Alket Mertiri, Theodore Hueckel, David J. D. Carter, "Self-Assembling Systems for Optical Out-of-Plane Coupling Devices," *ACS Nano,* 17, 3394-3400 (2023)

Theodore Hueckel, Diana J. Lewis, Alket Mertiri, David J. D. Carter, and Robert J. Macfarlane, "Controlling Colloidal Crystal Nucleation and Growth with Photolithographically Defined Templates," *ACS Nano 2023,* **17**, (21), 22121–22128 (2023)

## Honors and Awards

Nothing to report.

## Training Opportunities

This grant has trained one PhD student, Leo Zornberg, who led the optical characterization work, and one post-doc, Theodore Hueckl, who led the patterning work.

## Technology Transfer

One provisional US patent applications was filed by Draper:

Application No.: 63/570,374
Filing Date: 03/27/2024
Title: SELF-ASSEMBLED NANOPARTICLE MICROMIRRORS FOR OFF-CHIP OPTICAL COUPLING TOWAVEGUIDES
Inventors: David J. Carter; Sarah Geiger; Diana Lewis; Daniel Vresilovic

## Participants

| Name | Role | Person-Months |
|---|---|---|
| Carter, David J. | PI | 3 |
| Macfarlane, Robert | Faculty | 3 |
| Zornberg, Leo | Graduate Student/RA | 20 |
| Hueckl, Theodore | Post-doc | 22 |
| Lewis, Diana | Staff Scientist (doctoral) | 3 |
| Mertiri, Alket | Staff Scientist (doctoral) | 2 |
| Geiger, Sarah | Staff Scientist (doctoral) | 1 |

# REPORT DOCUMENTATION PAGE

| 1. REPORT DATE | 2. REPORT TYPE | 3. DATES COVERED | |
|---|---|---|---|
| | | START DATE | END DATE |
| 4/26/2024 | Final Research Performance Progress Report | 05/01/2019 | 04/30/2024 |

**4. TITLE AND SUBTITLE**

Nanoparticle-based Optical Components and Coatings (NOCC)

| 5a. CONTRACT NUMBER | 5b. GRANT NUMBER | 5c. PROGRAM ELEMENT NUMBER |
|---|---|---|
| | N00014-19-1-2213 | |
| **5d. PROJECT NUMBER** | **5e. TASK NUMBER** | **5f. WORK UNIT NUMBER** |
| | | |

**6. AUTHOR(S)**

Carter, David J.

| 7. PERFORMING ORGANIZATION NAME(S) AND ADDRESS(ES) | 8. PERFORMING ORGANIZATION REPORT NUMBER |
|---|---|
| CHARLES STARK DRAPER LABORATORY, IN<br>DRAPER LABORATORY<br>555 TECHNOLOGY SQ<br>CAMBRIDGE MA 02139-3539<br>UNITED STATES OF AMERICA | CSDL-001 |

| 9. SPONSORING/MONITORING AGENCY NAME(S) AND ADDRESS(ES) | 10. SPONSOR/MONITOR'S ACRONYM(S) | 11. SPONSOR/MONITOR'S REPORT NUMBER(S) |
|---|---|---|
| Office of Naval Research<br>875 N. Randolph St, Suite 1425<br>ARLINGTON VA 22203-1995 | ONR | |

**12. DISTRIBUTION/AVAILABILITY STATEMENT**

Approved for Public Release; Distribution is Unlimited.

**13. SUPPLEMENTARY NOTES**

**14. ABSTRACT**

We have shown that DNA-programmed assembly of nanoparticles on substrates can generate few-micron-scale Winterbottom crystal structures with well-known 3D shapes. We are using this as a building block to drive self-assembly to real-world applications of relevance to the Navy and the DoD. We are targeting DNA-nanoparticle (DNA-NP) crystal facets as micromirrors to propagate an optical signal from free space to a waveguide on a substrate. Such structures could be used for imaging and LiDAR, replacing low-efficiency and bandwidth-limited grating couplers with high-efficiency and high-bandwidth mirrors, enabling compact, flat optical systems to replace bulk optics.

We have shown that our assembled structures have facets that exhibit specular reflection at controlled angles with high efficiency, have demonstrated out-of-plane light coupling from a microscope objective to an optical fiber, and studied the physics of nucleation and growth of DNA-NP crystals on patterned substrates. We can grow single crystal structures where we want them and have developed a process to fabricate waveguides integrated with self-assembled mirrors to demonstrate off-chip optical coupling to waveguides.

This capability should enable greatly-improved integrated optical systems and reduce size, weight and power for DoD platforms. Improved understanding of the nucleation and growth of the DNA-NP structures should eventually allow further exploration of more complex assembled materials by varying DNA length and nanoparticle size to create Gradient-Index (GRIN) optical coatings with high effective index contrast, and eventually even more complex optical metamaterials.

| 15. SUBJECT TERMS | | | | |
|---|---|---|---|---|
| Self-assembly, DNA, optical coupling, integrated optics, nanoparticles, nanomaterials, optics, out-of-plane coupling, micromirror, lithography, crystallization kinetics, crystal patterning, directed assembly | | | | |
| **16. SECURITY CLASSIFICATION OF:** | | | **17. LIMITATION OF ABSTRACT** | **18. NUMBER OF PAGES** |
| **a. REPORT** | **b. ABSTRACT** | **C. THIS PAGE** | | |
| unclassified | unclassified | unclassified | UU | 12 |
| **19a. NAME OF RESPONSIBLE PERSON** | | | **19b. PHONE NUMBER** *(Include area code)* | |
| Carter, David J. | | | (617) 258 2079 | |